Effect of halogen doping on the electronic, electrical, and optical properties of anatase TiO$_2$

Petros-Panagis Filippatos, Nikolaos Kelaidis, Maria Vasilopoulou, et al.

open access

View Online   Export Citation   CrossMark

ARTICLES YOU MAY BE INTERESTED IN

First-principles quantum treatment of electron–phonon interactions in thin-film nanodevices
AIP Advances **12**, 115015 (2022); https://doi.org/10.1063/5.0124158

Advances in low dimensional and 2D materials
AIP Advances **12**, 110401 (2022); https://doi.org/10.1063/5.0129120

Optimization for energy response characteristics of plastic scintillators based on genetic algorithm
AIP Advances **12**, 115111 (2022); https://doi.org/10.1063/5.0124131

READ NOW!

AIP Advances

Energy Collection

AIP Publishing

Effect of halogen doping on the electronic, electrical, and optical properties of anatase TiO$_2$

View Online   Export Citation   CrossMark

Petros-Panagis Filippatos,[1,2,a)] (ID) Nikolaos Kelaidis,[3] Maria Vasilopoulou,[1] (ID) Dimitris Davazoglou,[1]
and Alexander Chroneos[4,5,a)]

AFFILIATIONS

[1] Institute of Nanoscience and Nanotechnology (INN), National Center for Scientific Research Demokritos,
15310 Agia Paraskevi, Athens, Greece
[2] Faculty of Engineering, Environment and Computing, Coventry University, Priory Street, Coventry CV1 5FB, United Kingdom
[3] Theoretical and Physical Chemistry Institute, National Hellenic Research Foundation, Vass. Constantinou 48,
GR-11635 Athens, Greece
[4] Department of Electrical and Computer Engineering, University of Thessaly, 38221 Volos, Greece
[5] Department of Materials, Imperial College, London SW7 2AZ, United Kingdom

[a)] Authors to whom correspondence should be addressed: filippap@coventry.ac.uk and alexander.chroneos@imperial.ac.uk

ABSTRACT

Titanium dioxide (TiO$_2$) is one of the most used oxides in renewable energy applications, such as hydrogen production, photovoltaics, and light-emitting diodes. To further improve the efficiency of the devices, doping strategies are used to modify their fundamental properties. Here, we used density functional theory (DFT) simulations to explore the effect of all the halogen dopants on the structural, electronic, and optical properties of TiO$_2$. We investigated both the interstitial and the oxygen substitutional positions, and for the optimized structures, we used hybrid DFT calculations to predict the electronic and optical properties. In all cases, we found that halogen dopants reduce the bandgap of the pristine TiO$_2$ while gap states also arise. The halogen dopants constitute a single acceptor when they occupy interstitial sites, while when they are inserted in oxygen sites, they act as donors. This can be established by the states that form above the valence band. It is proposed that these states contribute to the significant changes in the optical and electronic properties of TiO$_2$ and can be beneficial to the photovoltaic and photocatalytic applications of TiO$_2$. Importantly, the iodine doping of TiO$_2$ significantly reduces the bandgap of TiO$_2$ while increasing its dielectric constant, making it suitable for light-harvesting applications.

INTRODUCTION

TiO$_2$ is a semiconductor with n-type conductivity that crystallizes in anatase, rutile, and brookite structures.[1–6] Doping is considered an appropriate and low-cost method to increase the electrical conductivity and the transparency of TiO$_2$.[7–9] It is mainly used in solar cell technology as an electron transport layer material,[10] in photocatalysis for hydrogen production,[11] and in sensing applications.[12] Many experiments have investigated the halogen doping of TiO$_2$,[13–16] with fluorine being the most used dopant for optoelectrical applications.[17,18] As it is stated in these studies, fluorine doping modifies the properties of the bulk and the surface.[17,18] In particular, fluorine leads to highly crystalline and photoactive samples as it hampers the anatase to rutile phase transformation.[13] Fluorine also enables the formation of defects on the surface of anatase, and this leads to an improved absorption in the near-ultra-violet (UV) region and favors the formation of long-living luminescent surface trapping sites.[13] Wang et al.[19] investigated the photocatalytic activity of Cl:TiO$_2$ with various doping concentrations. Their results showed that the photocatalytic activity increases up to a level with respect to the Cl content. This is due to the additional energy levels formed in the bandgap when the surface Ti^{3+} exceeds a particular value. As a

result, higher Cl dopant results in excessive surface Ti^{3+}, which act as surface recombination centers for e^-/h^+ and accordingly suppress the photocatalytic activity.[19,20]

Regarding bromine doping, there are fewer reports that focus on the effect on TiO_2, but it was predicted that it reduces the bandgap of TiO_2 and the co-doping with chlorine enhances the photocatalytic activity.[21] The electronic and optical properties of $I:TiO_2$ were extensively investigated from an experimental point of view. In many works, it was determined that a profound gap reduction occurred due to iodine incorporation.[16,22,23] For example, Hong et al.[24] predicted that iodine doping of TiO_2 that is prepared with a hydrolysis method exhibited an efficient decomposition of phenol under constant visible irradiation.

Apart from the experimental results, density functional theory (DFT) studies also examine the effect of halogen doping in TiO_2. In their work, Yang et al.[25] investigated the role of halogen dopants in substitutional positions in TiO_2. They predicted that iodine reduces the bandgap from 3.16 to 2.50 eV. Notably, in their simulations, they used the "scissors operation" to tackle the well-known problem of gap underestimation.[26] Apart from the scissors operation, a variety of methods have been developed to correct the bandgap of TiO_2, such as the Hubbard + U method,[27] and the more computationally expensive hybrid pseudopotentials that produce the most accurate bandgap values.

Here, we employed hybrid DFT calculations to extensively investigate the effect of halogens in the bulk properties of TiO_2. Specifically, we examine the changes in the electronic and optical properties and the potential applications in photocatalysis and photovoltaics. In this perspective, we predicted a bandgap that reaches a value of 3.56 eV, agreeing with the experimental bandgap.[28] Herein, we have examined interstitial and substitutional defect sites, and for the minimum energy systems, we predicted the changes in the electronic, electrical, and optical properties. Using the total and partial density of states (pDOS), we analyzed the minimum sites and their effect on the energy gap. Furthermore, we have predicted the absorption for all the doping cases and we discuss our results with the available literature data.

METHODOLOGY

For our study, we used the Cambridge Serial Total Energy Package (CASTEP).[29,30] We employed the hybrid functional PBE0 to encounter the bandgap underestimation due to the effect of the
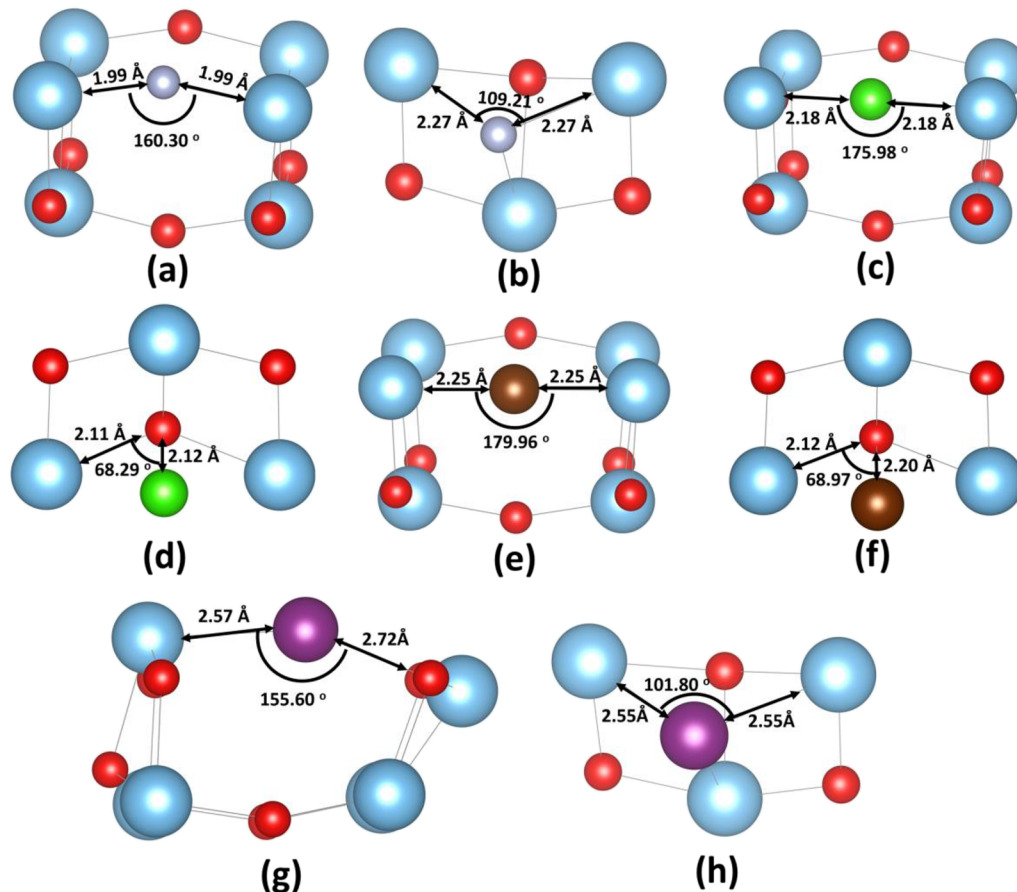

FIG. 1. The optimized structure of (a) $F_O:TiO_2$, (b) $F_i:TiO_2$, (c) $Cl_O:TiO_2$, (d) $Cl_i:TiO_2$, (e) $Br_O:TiO_2$, (f) $Br_i:TiO_2$, (g) $I_O:TiO_2$, and (h) $I_i:TiO_2$.

localized electrons.[31] We chose the cut-off energy at 800 eV for a supercell consisting of 48 atoms. In order to sample the first Brillouin zone during the geometry relaxation, we use a k-point mesh of $2 \times 2 \times 3$, while for the DOS calculations, we choose a set of $4 \times 4 \times 4$. Finally, the convergence criteria of our simulations were set at $2.0 \cdot 10^{-5}$ eV/atom for the SCF tolerance, 0.05 eV/Å for the force tolerance, and 0.001 Å for the max displacement tolerance. The analysis of the electronic bands and the semi-classical Boltzmann theory, to calculate the electrical conductivity, were employed using the BoltzTrap software.[32]

RESULTS

Structural properties

Anatase TiO_2 belongs to the I4/amd space group of the tetragonal system. The calculated lattice parameters of the unit cell are a = b = 3.74 Å and c = 9.45 Å, which are in good agreement with the experimental predicted values.[33] In Figs. 1(a)–1(h), the optimized dopant position in TiO_2 are presented. The introduction of dopants in the lattice creates local distortions, which translate to changes in the lattice parameters. The structural parameters are shown in Table I. In Fig. 2, we have plotted the change of the volume for each doping case, as a function of the radius of the dopant. The volume of the material increases with the increase of the dopant radius with $I:TiO_2$ having the highest volume.

Electrical properties

In Fig. 3, the DOS results for the halogen doped and undoped TiO_2 are presented. Generally, there are band structure changes in all the doping cases in interstitial and substitutional defects. In Fig. 3(i), we include as a reference the DOS of the undoped TiO_2 with a predicted gap value of 3.56 eV. This value agrees with previous experiments[28] and theoretical studies.[34] In particular, we predict a reduction to the bandgap, and specifically in the interstitial defects, energy levels near the conduction and the valence band are created. In Fig. 3(a), the DOS of $Fo:TiO_2$ is shown. It is seen that the F substitutional does not exhibit any energy states inside the gap, but it slightly decreases the gap to 3.43 eV. Conversely, interstitial doping [Fig. 3(b)] gives rise to gap states near the conduction and the valence band edges. In this case, the bandgap is significantly reduced to a value of 3.15 eV. For the Cl doping, we can
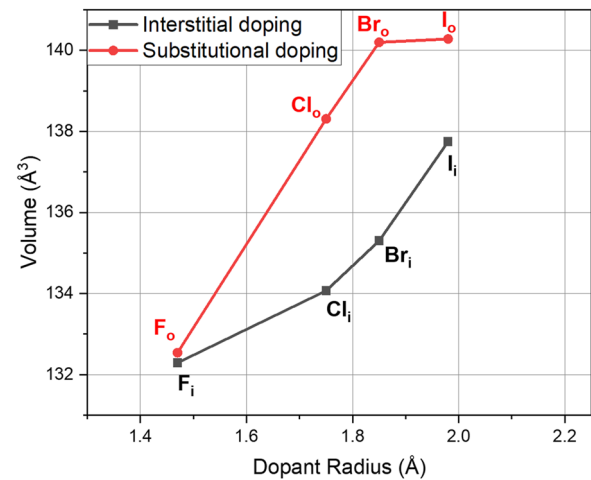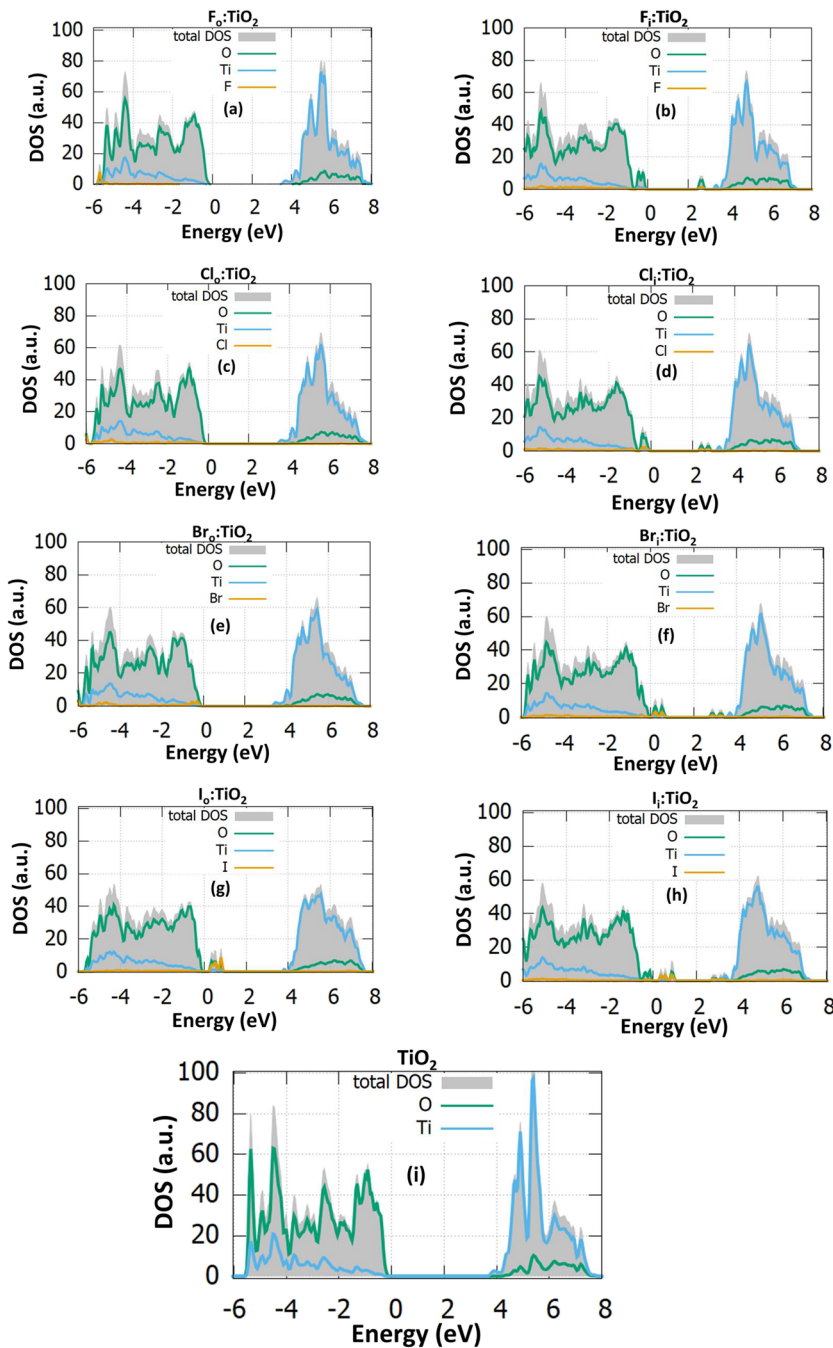

FIG. 2. Increase in the volume of TiO_2 due to the halogen dopants.

see that in the substitution of oxygen the bandgap is again reduced to a value of 3.33 eV, while in the interstitial position, it reaches the value of 3.09 eV. Similar to the fluorine case, we can predict the formation of energy states at the edge of the conduction band. In previous work on F and Cl doping, we also observed a significant reduction in the case of chlorine doping even at lower dopant contents.[27,35]

Regarding bromine doping, we predict that the $Br_O:TiO_2$ has a bandgap value of 3.24 eV, while interstitial doping significantly reduces the gap at a value of 2.70 eV. Again, gap states are formed near the valence band, which are mainly attributed to bromine as well as near the conduction band with the contribution of oxygen and bromine. The case is quite different with iodine dopant. Interestingly, when inserted as a substitute for oxygen, it increases the bandgap to a value of 3.65 eV. This time, the $I_O:TiO_2$ exhibits additional energy levels near the valence band maximum (VBM). Such states near the oxide's VBM and those near the conduction band can act as shallow and deep acceptors, respectively, hence contributing to the performance of solar-cell devices based on TiO_2. Conversely, the interstitial doping reduces the bandgap to a value of 2.66 eV and mid-gap states are formed. These states can also act

TABLE I. The lattice parameters after geometry relaxation for every examined dopant.

	a (Å)		c (Å)		Volume (Å^3)	
	Interstitial	Substitutional	Interstitial	Substitutional	Interstitial	Substitutional
F:TiO$_2$	3.72	3.76	9.56	9.40	132.29	132.54
Cl:TiO$_2$	3.75	3.84	9.56	9.38	134.07	138.31
Br:TiO$_2$	3.76	3.86	9.57	9.41	135.30	140.20
I:TiO$_2$	3.79	3.77	9.59	9.87	137.75	140.28
Undoped	3.74		9.45		132.18	

FIG. 3. The density of states graphs for (a) F_O:TiO$_2$, (b) F_i:TiO$_2$, (c) Cl_O:TiO$_2$, (d) Cl_i:TiO$_2$, (e) Br_O:TiO$_2$, (f) Br_i:TiO$_2$, (g) I_O:TiO$_2$, (h) I_i:TiO$_2$, and (i) the undoped.

as traps for the photogenerated carriers leading to a decrease in the device photocurrent and efficiency. The present results considering the F, Cl, Br, and I substitutes are consistent with the work of Yang *et al.*[25] regarding the decrease of the forbidden bandgap. Nevertheless, using the hybrid functionals, we obtain different results for I substitutional doping, where we see both the bandgap to increase and the formation of donor-type states.

Generally, we conclude that the substitutional doping of halogen atoms does not introduce any available energy levels, with iodine being an exception. This contrasts with the interstitial dopants that change the edges both in the valence and conduction band. This strongly suggests the presence of free electrons that enhance the n-type conductivity of TiO$_2$ and has also been observed in other similar oxides, such as SnO$_2$.[36]

**TABLE II.** The bandgap values for every halogen doped TiO$_2$.

	Bandgap (eV)	
	Interstitial	Substitutional
F:TiO$_2$	3.15	3.43
Cl:TiO$_2$	3.09	3.33
Br:TiO$_2$	2.70	3.24
I:TiO$_2$	2.66	3.65
Undoped	3.56	

In Table II, we have summarized the bandgap values for all the doping cases. The lowest bandgap is achieved with I$_i$:TiO$_2$ and Br$_i$:TiO$_2$. In the case of I$_o$:TiO$_2$ at a doping percentage of 2.08%, we can see the highest gap value. Therefore, it is proposed that iodine doping at these doping percentages should be examined as an electron transport layer in photovoltaics, while bromine should also be examined as a dopant to develop better photocatalysts.

In Fig. 4, the projected DOS for the interstitial doped cases are examined. Through the pDOS, we can decode the hybridization of the orbitals that create the gap states. As we show in Fig. 4(a), F doping has new additional energy levels near the conduction band edge. The states located at 2.5 eV arise due to the hybridization of

O-2p with F-2p orbitals. In the case of chlorine, it is seen that the Cl-3p orbitals contribute to the gap states near the valence and the conduction band. We also observe the same in the bromine interstitial where the states occur because of the hybridization of Br-4p and O-2p orbitals. Finally, in the case of iodine interstitial, the inner gap states arise at 0.2 eV due to the hybridization of I-5p, Ti-3d, and O-2p. The present results agree with previous DFT work on halogen doped SnO$_2$, which in turn indicates that the formation of gap states in halogen doped oxides may have a universal origin.[37]

To further investigate the electrical properties of halogen doped anatase TiO$_2$, such as the electrical conductivity, the BoltzTrap code,[32] which is based on the semiclassical Boltzmann transport equation, was used for each dopant in both interstitial and substitutional positions. To gain a better insight into the electrical conductivity changes, we predict the conductivity value at the Fermi level at 300 K. The electrical conductivity estimates the flow of free charge carriers (e$^-$/h$^+$ pairs) inside the bulk structure as a function of temperature and chemical potential. The calculated electrical conductivity to scattering time (σ/τ) of halogen doped TiO$_2$ is presented in Fig. 5, while the results for the undoped agree with the available literature.[38–40] We predict a reduction of the conductivity with the increase of the temperature for every case. We can see that both in the substitutional and interstitial doping, bromine and iodine have shown interesting results as they have improved the conductivity in the n-type area of the chemical potential. In Table III, we have collected all the conductivity values at the
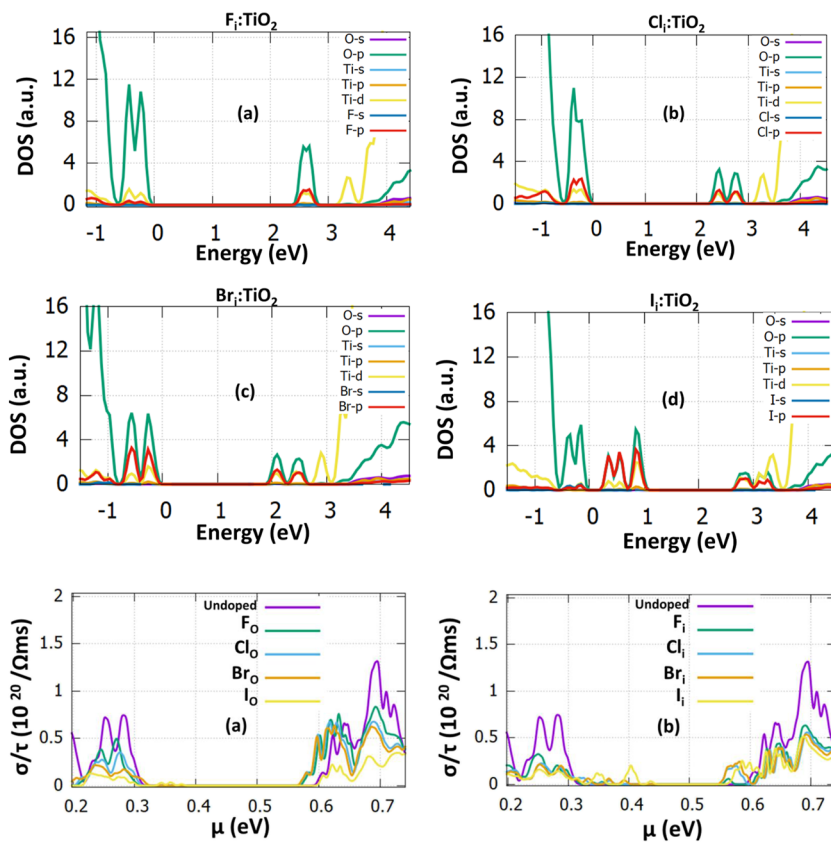
FIG. 4. The projected density of states graphs for (a) F$_i$:TiO$_2$, (b) Cl$_i$:TiO$_2$, (c) Br$_i$:TiO$_2$, and (d) I$_i$:TiO$_2$.

FIG. 5. The conductivity graphs for (a) substitutional and (b) interstitial doping. The conductivity of the undoped is presented with purple for reference.

TABLE III. The conductivity to scattering time values for every halogen doped TiO$_2$ in the conduction band edge.

	Conductivity to scattering time (S/ms)	
	Interstitial	Substitutional
F:TiO$_2$	0.20×10^5	0.74×10^5
Cl:TiO$_2$	0.66×10^5	0.78×10^5
Br:TiO$_2$	0.97×10^5	0.91×10^5
I:TiO$_2$	0.10×10^6	0.47×10^5
Undoped	0.79×10^5	

conduction band edge, where significant changes are predicted for each compound. This improvement of conductivity is beneficial for applying halogen doping on modern solar cells. The increase in the case of iodine interstitial is of great importance, and it opens the road to the application of I:TiO$_2$ to photovoltaics as an electron transport layer or to sensors as a primary sensing material. Furthermore, improvements may be achieved by co-doping strategies and processing conditions as has been previously demonstrated in related materials.[41,42]

Optical properties

Finally, in Fig. 6, the absorption coefficiency is presented for the undoped and doped samples. All the cases considered here have an absorption range in the ultraviolet light region. Compared to the undoped cases, we predicted that, in the interstitial doping [Fig. 6(a)], the absorbance is significantly enhanced with the I$_i$:TiO$_2$ having the highest absorbance among the other dopants. In the case of substitutional doping [Fig. 6(b)], I and Br doping again show an improvement to the absorbance compared to the other halogens or the undoped TiO$_2$. The present results for the absorbance of undoped TiO$_2$ agree well with previous DFT[43] and experimental studies.[44] From the optical results, it can be concluded that when halogens incorporate oxygen sites, it is more beneficial for applying TiO$_2$ to photovoltaic technologies. This can be achieved when the dopant is inserted in a small amount where it sitsite in an oxygen vacancy site. However, when the dopant is experimentally inserted in a large amount then due to the increase of the absorption it is more practical to be examined for alternative energy production, such as hydrogen production. Previous studies have shown that a high percentage of doping significantly improves the photocatalytic properties of TiO$_2$ and thus the hydrogen production.[28]

CONCLUSION

In this work, we used DFT to predict the changes of the structural, electrical, and optical properties of TiO$_2$ due to halogen doping. In all the examined cases, we predicted that the halogen incorporation significantly reduces the bandgap, except for the case of iodine, where when inserted as an oxygen substitutional it increases the bandgap. We also predicted the electrical conductivity of interstitial and substitutional doping and we found that iodine and bromine significantly enhance it. Finally, we predicted that halogens improve the absorbance of TiO$_2$. Interestingly, iodine doping has the highest absorbance among the other halogens, making it the most suitable dopant candidate for light-harvesting applications.

AUTHOR DECLARATIONS

Conflict of Interest

The authors have no conflicts to disclose.

Author Contributions

Petros-Panagis Filippatos: Conceptualization (equal); Data curation (equal); Formal analysis (equal); Investigation (equal); Methodology (equal). **Nikolaos Kelaidis**: Investigation (equal); Methodology (equal); Visualization (equal). **Maria Vasilopoulou**: Methodology (equal); Resources (equal); Supervision (equal); Visualization (equal). **Dimitris Davazoglou**: Data curation (equal); Supervision (equal). **Alexander Chroneos**: Funding acquisition (equal); Methodology (equal); Software (equal); Supervision (equal).
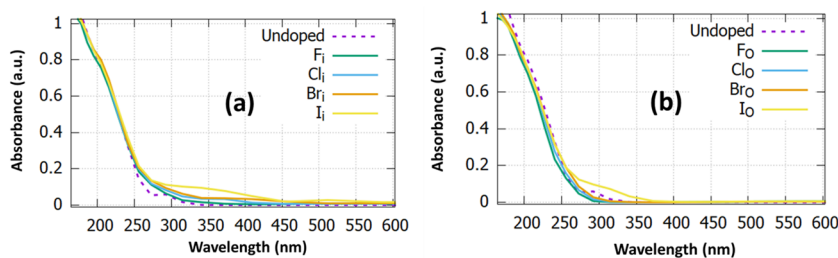
FIG. 6. The absorption coefficiency for (a) the undoped and (b) doped samples.

DATA AVAILABILITY

The data that support the findings of this study are available within the article.

REFERENCES

[1] A. Fujishima and K. Honda, Nature **238**(5358), 37 (1972).

[2] M. Grätzel, Nature **414**, 338–344 (2001).

[3] R. Asahi, T. Morikawa, T. Ohwaki, K. Aoki, and Y. Taga, Science **293**, 269–271 (2001).

[4] S. U. M. Khan, M. Al-Shahry, and W. B. Ingler, Science **297**, 2243–2245 (2002).

[5] S. P. Russo, I. E. Grey, and N. C. Wilson, J. Phys. Chem. C **112**, 7653–7664 (2008).

[6] H. G. Yang, C. H. Sun, S. Z. Qiao, J. Zou, G. Liu, S. C. Smith, H. M. Cheng, and G. Q. Lu, Nature **453**, 638–641 (2008).

[7] M. Okutan, E. Basaran, H. I. Bakan, and F. Yakuphanoglu, Physica B **364**, 300–305 (2005).

[8] C. Di Valentin, E. Finazzi, G. Pacchioni, A. Selloni, S. Livraghi, M. C. Paganini, and E. Giamello, Chem. Phys. **339**, 44–56 (2007).

[9] P. S. Basavarajappa, S. B. Patil, N. Ganganagappa, K. R. Reddy, A. V. Raghu, and C. V. Reddy, Int. J. Hydrogen Energy **45**, 7764–7778 (2020).

[10] M. Vasilopoulou, N. Kelaidis, E. Polydorou, A. Soultati, D. Davazoglou, P. Argitis, G. Papadimitropoulos, D. Tsikritzis, S. Kennou, F. Auras, D. G. Georgiadou, S.-R. G. Christopoulos, and A. Chroneos, Sci. Rep. **7**, 17839 (2017).

[11] P.-P. Filippatos, N. kelaidis, M. Vasilopoulou, D. Davazoglou, and A. Chroneos, Sci. Rep. **11**, 13031 (2021).

[12] B. Karunagaran, P. Uthirakumar, S. J. Chung, S. Velumani, and E.-K. Suh, Mater. Charact. **58**, 680–684 (2007).

[13] M. V. Dozzi, C. D'Andrea, B. Ohtani, G. Valentini, and E. Selli, J. Phys. Chem. C **117**, 25586–25595 (2013).

[14] M. Long, W. Cai, H. Chen, and J. Xu, Front. Chem. China **2**, 278–282 (2007).

[15] Y.-H. Zhang, M.-J. Li, H.-J. Wang, R. Yuan, and S.-P. Wei, Anal. Chem. **91**, 10864–10869 (2019).

[16] S. Tojo, T. Tachikawa, M. Fujitsuka, and T. Majima, J. Phys. Chem. C **112**, 14948–14954 (2008).

[17] J. Song, H. B. Yang, X. Wang, S. Y. Khoo, C. C. Wong, X.-W. Liu, and C. M. Li, ACS Appl. Mater. Interfaces **4**, 3712–3717 (2012).

[18] S. I. Noh, K.-N. Bae, H.-J. Ahn, and T.-Y. Seong, Ceram. Int. **39**, 8097–8101 (2013).

[19] X.-K. Wang, C. Wang, W.-Q. Jiang, W.-L. Guo, and J.-G. Wang, Chem. Eng. J. **189–190**, 288–294 (2012).

[20] S. Ikeda, N. Sugiyama, S.-y. Murakami, H. Kominami, Y. Kera, H. Noguchi, K. Uosaki, T. Torimoto, and B. Ohtani, Phys. Chem. Chem. Phys. **5**, 778–783 (2003).

[21] H. Luo, T. Takata, Y. Lee, J. Zhao, K. Domen, and Y. Yan, Chem. Mater. **16**, 846–849 (2004).

[22] W. Deng, S. Ning, Q. Lin, H. Zhang, T. Zhou, H. Lin, J. Long, Q. Lin, and X. Wang, Colloids Surf., B **144**, 196–202 (2016).

[23] G. Liu, Z. Chen, C. Dong, Y. Zhao, F. Li, G. Q. Lu, and H.-M. Cheng, J. Phys. Chem. B **110**, 20823–20828 (2006).

[24] X. Hong, Z. Wang, W. Cai, F. Lu, J. Zhang, Y. Yang, N. Ma, and Y. Liu, Chem. Mater. **17**, 1548–1552 (2005).

[25] K. Yang, Y. Dai, B. Huang, and M.-H. Whangbo, Chem. Mater. **20**, 6528–6534 (2008).

[26] L. J. Sham and M. Schlüter, Phys. Rev. Lett. **51**, 1888 (1983).

[27] P.-P. Filippatos, N. Kelaidis, M. Vasilopoulou, D. Davazoglou, N. N. Lathiotakis, and A. Chroneos, Sci. Rep. **9**, 19970 (2019).

[28] P.-P. Filippatos, A. Soultati, N. Kelaidis, C. Petaroudis, A.-A. Alivisatou, C. Drivas, S. Kennou, E. Agapaki, G. Charalampidis, A. R. b. M. Yusoff, N. N. Lathiotakis, A. G. Coutsolelos, D. Davazoglou, M. Vasilopoulou, and A. Chroneos, Sci. Rep. **11**, 5700 (2021).

[29] M. C. Payne, M. P. Teter, D. C. Allan, T. A. Arias, and J. D. Joannopoulos, Rev. Mod. Phys. **64**, 1045–1097 (1992).

[30] M. D. Segall, P. J. D. Lindan, M. J. Probert, C. J. Pickard, P. J. Hasnip, S. J. Clark, and M. C. Payne, J. Phys.: Condens. Matter **14**, 2717–2744 (2002).

[31] J. Paier, M. Marsman, K. Hummer, G. Kresse, I. C. Gerber, and J. G. Ángyán, J. Chem. Phys. **124**, 154709 (2006).

[32] G. K. H. Madsen and D. J. Singh, Comput. Phys. Commun. **175**, 67–71 (2006).

[33] J. K. Burdett, T. Hughbanks, G. J. Miller, J. W. Richardson, Jr., and J. V. Smith, J. Am. Chem. Soc. **109**, 3639–3646 (1987).

[34] M. Landmann, E. Rauls, and W. G. Schmidt, J. Phys.: Condens. Matter **24**, 195503 (2012).

[35] W. Li, Phys. Status Solidi RRL **9**(1), 10–27 (2015).

[36] L. Chinnappa, K. Ravichandran, K. Saravanakumar, G. Muruganantham, and B. Sakthivel, J. Mater. Sci.: Mater. Electron. **22**, 1827–1834 (2001).

[37] P.-P. Filippatos, N. Kelaidis, M. Vasilopoulou, D. Davazoglou, and A. Chroneos, Appl. Sci. **11**, 551 (2021).

[38] G. K. H. Madsen, J. Carrete, and M. J. Verstraete, Comput. Phys. Commun. **231**, 140–145 (2018).

[39] A. Soussi, A. A. Hssi, M. Boujnah, L. Boulkadat, K. Abouabassi, A. Asbayou, A. Elfanaoui, R. Markazi, A. Ihlal, and K. Bouabid, J. Electron. Mater. **50**, 4497–4510 (2021).

[40] W. Naffouti, T. Ben Nasr, H. Meradji, and N. Kamoun-Turki, J. Electron. Mater. **45**, 5096–5103 (2016).

[41] N. kelaidis, A. Kordatos, S.-R. G. Christopoulos, and A. Chroneos, Sci. Rep. **8**, 12790 (2018).

[42] C. Petaroudis, I. Kostis, P.-P. Filippatos, A. Chroneos, A. Soultati, M. Vasilopoulou, and D. Davazoglou, Thin Solid Films **741**, 139039 (2022).

[43] M. Harb, J. Phys. Chem. C **117**, 12942–12948 (2013).

[44] K. Huang, L. Chen, J. Deng, and J. Xiong, J. Nanomater. **2012**, 720491.